Pulsed nuclear double resonance in impurity-doped ionic crystals

Toshihiko Taki* and Mitsuo Satoh
Technical College, Tokushima University, Tokushima 770, Japan
and Faculty of Engineering, Tokushima University, Tokushima 770, Japan
(Received 6 June 1980)

The highly sensitive nuclear magnetic double-resonance technique has been used to study the first- and second-order quadrupole interactions of nuclear magnetic resonance lines due to the nuclei surrounding the substitutional impurity ions in ionic crystals. By studying the rotational pattern of the quadrupole spectra, signals observed are assigned to (1,0,0)-, (1,1,0)-, and (1,1,1)-site nuclei around the doped impurity ions in NaCl, NaI, and NaBr single crystals. The principal values and the asymmetry parameters of the field gradients were found by using the quadrupole frequency obtained from the present study and the nuclear quadrupole moment for the nuclei under study. The asymmetry parameters of the field gradients at every (1,1,0) site in NaCl-Br, NaCl-I, NaCl-K, NaBr-Cl, and NaBr-I crystals have the same value, 0.10 within the experimental errors, with the same assignment of the principal axes.

I. INTRODUCTION

In perfect alkali halide crystals the quadrupole interaction of nuclei with spin greater than $\frac{1}{2}$ is zero because the electric field gradient (EFG) tensor at any sites vanishes due to the cubic symmetry of the lattice. However, for nuclei in the vicinity of impurities the symmetry is lowered and the resulting EFG gives rise to a quadrupole interaction. Various investigators[1–8] have studied the effects of impurity ions added to ionic crystals on the nuclear magnetic resonance (NMR) amplitude and linewidth. In order to get some idea of the magnitude of the EFG at a certain distance from the impurity, an "all-or-nothing" model proposed initially by Bloembergen and Rowland[1] in connection with metals has been employed in these studies. This relates the number of nuclei which are so near to the impurity that their satellites are perturbed by an amount greater than the magnetic resonance width, to the concentration of impurities and the line intensity. This model is not sufficiently precise for determination of the EFG at individual sites, and only gives an indication for sites existing farther than several lattice spacings from impurity.

Andersson[9–11] and Ohlsen and Melich[12] have successfully observed the second-order quadrupole shifts of the central line in impurity-doped alkali halide crystals using conventional broad-line NMR spectrometer. In experiments of this type the nuclei observed must have large quadrupole moments and large EFG's so that the central line is displaced sufficiently from the unperturbed central position, due to the second-order quadrupole interaction. However, owing to dislocations which are present in all "perfect" crystals and poor signal-to-noise ratio, it has been impossible to observe the satellite lines due to the first-order quadrupole splittings.

Since 1962, a pulsed nuclear magnetic double resonance (DNMR) technique introduced by Hartmann and Hahn[13] and modified by Lurie and Slichter[14] has been available, which enables us to observe a small number of nuclei. In favorable case it would be possible to detect the resonance of the nuclei as few as 10^{15} spins/cm^3. This technique was applied to the study of pure quadrupole interaction due to impurity ions in alkali halide crystals by Slusher and Hahn,[15,28] and to the study of the quadrupole interactions in copper containing zinc impurity ions, in zero magnetic field by Redfield.[16] This method has an advantage that the samples need only to be in the form of powder, but also the disadvantage that one cannot determine which sites are contributing to the resonance, and cannot decide the principal values and directions of principal axes of EFG tensors.

Recently, the experiments of DNMR in high magnetic field[17–26] have also been performed on alkali halide single crystals doped with a very low concentration of the impurities, in which one can determine the lattice sites contributing to the resonance and obtain the magnitudes and orientations of EFG tensors.

In this paper, a DNMR technique is used to study the first- and second-order quadrupole shifts of the nuclei which surround a substitutional impurity ion in alkali halide single crystals. Since we can definitely identify the lattice position of nuclei whose double resonance we observed, relative to the impurity, this experiment provides a partial map of the variation of the EFG near the impurity ions.

Section II describes the experimental technique and process, and Sec. III contains the presentation of data

obtained from the experiments and analysis of them. Finally, in Sec. IV a summary is given and the experimental values of EFG's and their asymmetry parameters are listed in Table I of this last section.

Comparison of the empirical results in this study with the calculations will be done in our coming paper.[27]

II. EXPERIMENTAL DETAILS

In the present study, the I spin system corresponds to the abundant Na nuclei remote from the impurity ions, while the I' spin system corresponds to the rare quadrupole-affected nuclei near the doped impurity ions.

The apparatus used for the measurements is a low-power cross-coil pulsed-NMR spectrometer which has been fully described previously[26] and required only minor modification during this work. A single transmitter coil is bimodally tuned to the Larmor frequencies of the I and I' spin systems. The block diagram is shown in Fig. 1.

All experiments are performed at 77 K and the probe is immersed in the bath of liquid nitrogen at atmospheric pressure. The experimental procedure was described elsewhere.[26]

The sample size was about $7 \times 7 \times 16$ mm^3 for all the crystals. All crystals except NaCl-I were grown from the reagent-grade powder doped with impurity ions by Kyropoulos method.

III. EXPERIMENTAL RESULTS

A. NaCl-Br crystal

An example of the DNMR spectra is shown in Fig. 2 for a NaCl single crystal containing 0.12 mole% Br^- impurities. The separation of the resonance lines is fairly good in this particular case where the angle θ between static magnetic field H_0 and the [001] crystal axis is 20°. Here M_I and M_{I0} represent the amplitude of the I spin free induction decay at the end of the measuring period with and without, respectively, heating rf pulse, and $\Delta\nu = \nu_m - \nu_L$ expresses the separation between the satellite frequency ν_m ($m = \frac{3}{2}$) and the Larmor ν_L for the I' spin system. By rotating H_0 about the [100] axis, we obtain the angular dependence of the quadrupole splittings shown in Fig. 3. As shown below, the observed an-

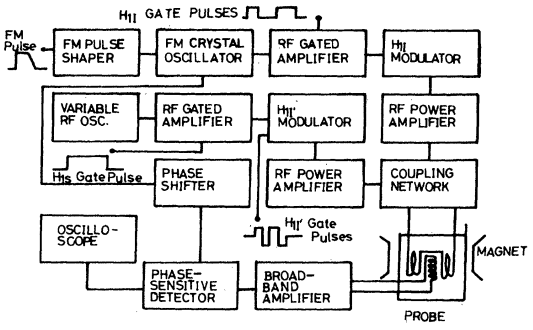

FIG. 1. Block diagram of DNMR spectrometer.

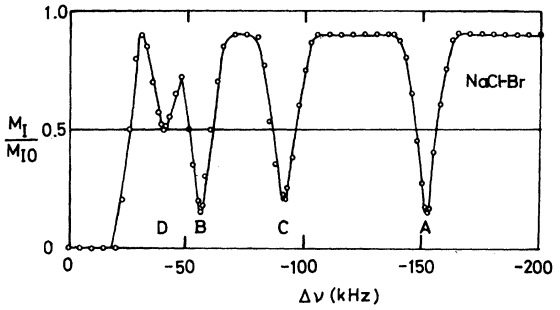

FIG. 2. DNMR spectrum ascribed to (1,0,0)- and (1,1,1)-sites Na in the vicinity of Br ions in NaCl crystal containing 0.125 mole% Br impurity ions at $\theta = 20°$, where θ is the angle between the static magnetic field H_0 and the [001] crystal axis. The $\Delta\nu = \nu_m - \nu_L$ represents the difference between the satellite frequency ν_m ($m = \frac{3}{2}$ or $-\frac{3}{2}$) and the Larmor ν_L for the I' spin system, and M_I and M_{I0} express the free induction decay amplitudes of the I spins at the end of measuring periods with and without, respectively, heating rf pulses.

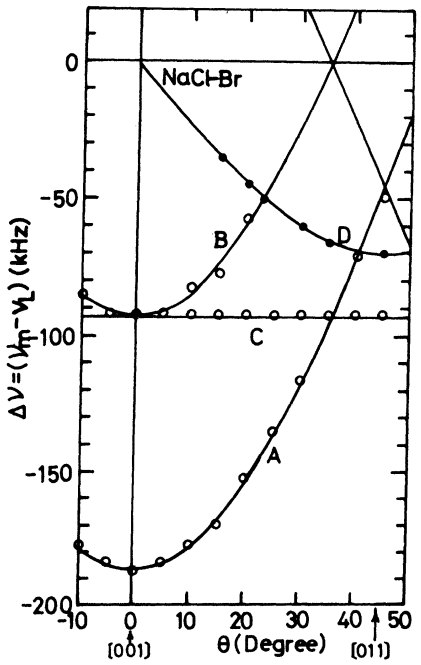

FIG. 3. Rotational pattern of the quadrupole spectra ascribed to (1,0,0)- and (1,1,1)-sites Na in the vicinity of Br ions in NaCl crystal containing 0.125 mole% Br impurity ions. The solid curves are calculated from Eqs. (1) and (2).

gular variation leads us to the assignment that these lines labeled as A, B, and C are considered to be associated with Na nuclei at $(A,0,0)$ sites relative to the added impurity ion at (0,0,0) site and with a unit of the interatomic distance of alkali halide crystals and the line labeled as D is due to (A,A,A) sites Na, where $A=1,3,\ldots$. A search for farther-remote satellites from the center line was performed up to $\Delta\nu=400$ kHz at $\theta=45°$, and no other lines were found. Therefore, these lines A, B, and C will be assigned to (1,0,0)-type Na and also the D to (1,1,1)-type Na. The signals due to (3,0,0) or (3,3,3) Na are considered to be masked under the spread of the central line ($m=+\frac{1}{2}\leftrightarrow-\frac{1}{2}$) and will not be observed because of the smaller distortion compared with the (1,0,0)- and (1,1,1)-type Na. For (1,0,0) sites, the angular variation of the quadrupole splittings for $m=-\frac{3}{2}\leftrightarrow-\frac{1}{2}$ and $m=\frac{3}{2}\leftrightarrow\frac{1}{2}$ transitions in the first-order perturbation[29,30] is given by

$$\Delta\nu(A)=\mp\nu_Q(1+3\cos2\theta)/4\ ,$$
$$\Delta\nu(B)=\mp\nu_Q(1-3\cos2\theta)/4\ , \qquad (1)$$
$$\Delta\nu(C)=\pm\nu_Q/2\ ,$$

where $\nu_Q=e^2qQ/2h$ is the quadrupole frequency, eq is the EFG at the nucleus in question, Q is the quadrupole moment of the nucleus under study, and h is the Planck's constant. Also for (1,1,1) site nucleus we have[29,30]

$$\Delta\nu(D)=\mp\nu_Q(\sin2\theta)/2\ . \qquad (2)$$

The asymmetry parameter of the EFG, η, is zero for these sites. The solid curves in Fig. 3 are described by Eqs. (1) and (2) assuming $\nu_Q=187.7$ kHz for A, B, C and $\nu_Q=140$ kHz for D lines, respectively, so as to get the best fits with the experimental values. The same spectra as Fig. 3 were obtained by using NaCl single crystals containing 0.25, 0.33, 0.5, or 1 mole% Br^-. For comparison, a pure NaCl crystal was examined and no satellite lines were found in the range of $\Delta\nu$ from 40 to 430 kHz. Slusher and Hahn[28] made the very sensitive experiments of pure quadrupole resonance (PQR) by using DNMR. They obtained $\nu_Q=191.5$ kHz for their observed B signal in NaCl containing Br^- impurity ions without assignment of nuclear sites and species. The ν_Q of Na (1,0,0) in the present study agrees fairly well with that of B signal. But the ν_Q in this study does not agree with the results of Kawamura *et al.*[4] ($\nu_Q=248$ kHz at 300 K) and Andersson[11] ($\nu_Q=350$ kHz at 100 K) for Na (100) site.

Also the signals due to the $(A,A,0)$-type Cl are observed. By rotating the magnetic field H_0 about the [100] crystal axis, we obtain the angular dependence of the quadrupole spectra, an example of which is shown in Fig. 4. The rotation pattern for the NaCl-Br crystal as shown in Fig. 5 is the usual one encountered when we observe the quadrupole spectra of nuclei at $(A,A,0)$ position with respect to the substitutional impurity ions at (0,0,0) where $A=1,3,\ldots$. Since no other signals were observed in the range of $\Delta\nu=\pm1.6$ MHz, the observed signal will be due to the Cl (1,1,0). The angular variations of the quadru-

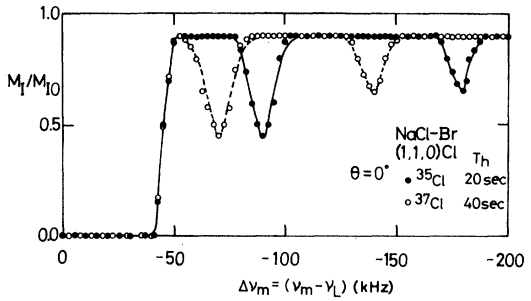

FIG. 4. DNMR spectrum ascribed to (1,1,0)-site Cl in the vicinity of Br ions in NaCl crystal containing 0.125 mole% Br impurity ions. The T_h represents the heating time of the I' spins by the rf pulse.

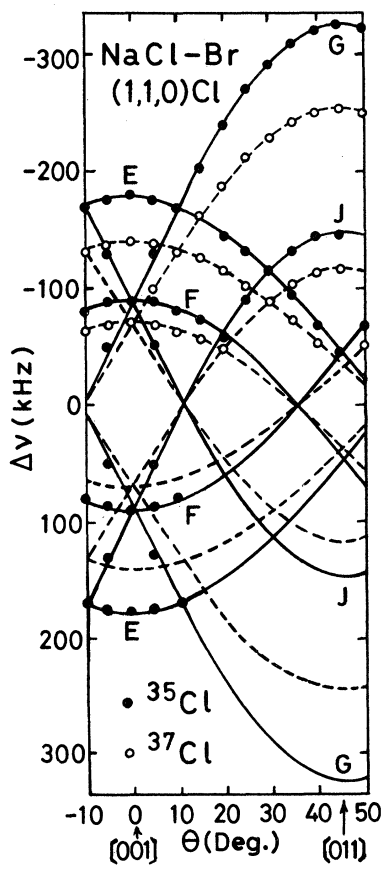

FIG. 5. Angular variation of the quadrupole spectra ascribed to Cl (1,1,0) in the vicinity of Br impurity ions in NaCl crystal. The solid and dashed lines are calculated from Eqs. (3).

pole splittings for $m=-\frac{3}{2}\leftrightarrow-\frac{1}{2}$ and $\frac{3}{2}\leftrightarrow\frac{1}{2}$ transitions in the first-order perturbation[29,30] are given by

$$\begin{aligned}\Delta\nu(E)&=\pm\nu_Q(1+\eta)(1-3\cos2\theta)/8\ ,\\ \Delta\nu(F)&=\pm\nu_Q(1+\eta)(1+3\cos2\theta)/8\ ,\\ \Delta\nu(G)&=\mp\nu_Q[(1+\eta)+(3-\eta)\sin2\theta]/4\ ,\\ \Delta\nu(J)&=\mp\nu_Q[(1+\eta)-(3-\eta)\sin2\theta]/4\ ,\end{aligned}\tag{3}$$

where η is the asymmetry parameter. From the analysis of the spectra we obtain $\nu_Q=(325.0\pm2.0)$ and (254.0 ± 2.0) kHz for ^{35}Cl and ^{37}Cl, respectively, and the asymmetry parameter of EFG, $\eta=(0.105\pm0.005)$ for both nuclei. From these results, the ratio of ν_Q^{37}/ν_Q^{35} is 0.782 which agrees with that of the nuclear quadrupole moments, Q^{37}/Q^{35}. Using $Q^{37}=-0.0621\times10^{-24}$ cm^2 and $Q^{35}=-0.0789\times10^{-24}$ cm^2, we have the principal values of the EFG: $V_{xx}=\mp50.6\times10^{12}$ esu/cm^3, $V_{yy}=\mp62.4\times10^{12}$ esu/cm^3, and $V_{zz}\equiv eq_{\rm exp}=\pm113\times10^{12}$ esu/cm^3 with the directions of the principal axes x, y, and z relative to the crystal axes

x: $(1,\bar{1},0)$, y: $(0,0,1)$, z: $(1,1,0)$

or

x: $(1,1,0)$, y: $(0,0,1)$, z: $(1,\bar{1},0)$,

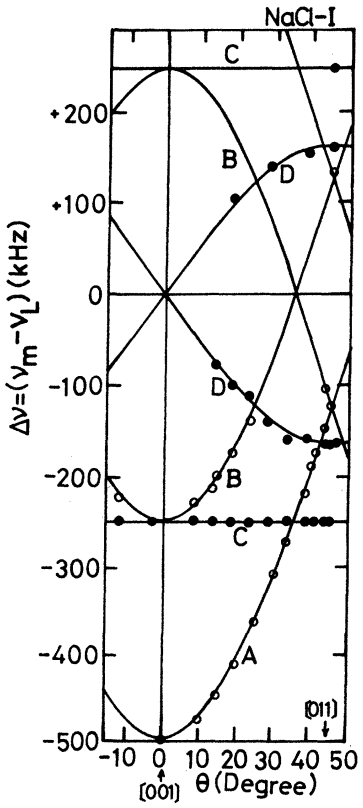

FIG. 6. Rotational pattern of the quadrupole spectra ascribed to Na (1,0,0) and (1,1,1) sites in the vicinity of I ions in NaCl crystal containing 0.278 mole% I impurity ions. The solid curves are calculated from Eqs. (1) and (2).

where (i,j,k) represents the direction cosines. In addition, the spectra for positive $\Delta\nu$ were checked, and both quadrupole spectra with positive and negative $\Delta\nu$ were symmetrical with respect to the central frequency $\nu_{I'0}$ within experimental errors.

B. NaCl-I crystal

By rotating H_0 about the [100] crystal axis, we obtain the angular dependence of the quadrupole spectra as shown in Fig. 6 for the NaCl single crystal containing 0.278 mole% I^- impurity ions. Following the arguments of Sec. III A, the lines labeled as A, B, and C are considered to be due to Na (1,0,0), and line D to Na (1,1,1). The search field frequency $\nu_{I'}$ was extended to $\Delta\nu=\pm1$ MHz at $\theta=45°$ and no other satellites were found. The lines A, B, and C are found to fit Eqs. (1) with $\nu_Q=500$ kHz and D to fit Eq. (2) with $\nu_Q=330$ kHz. In addition, the spectra for posi-

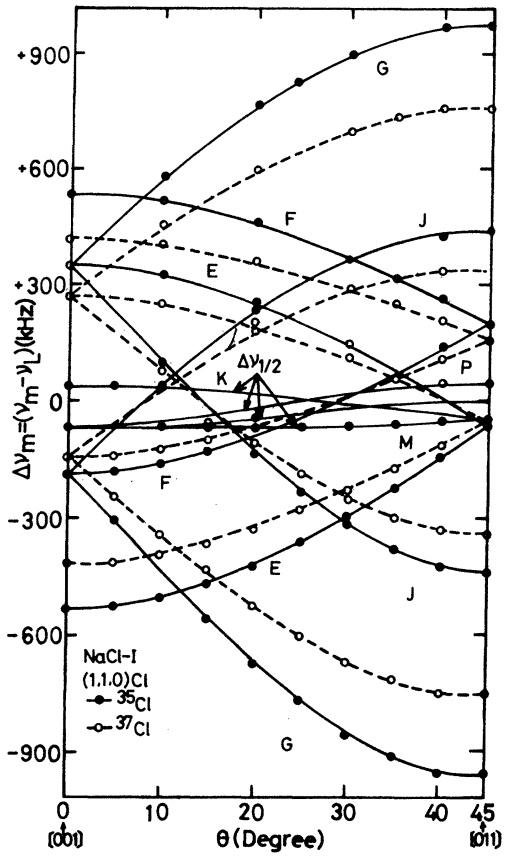

FIG. 7. Angular variation of the quadrupole spectra ascribed to Cl (1,1,0) in the vicinity of I ions in NaCl crystal containing 0.278 mole% I impurity ions. The solid and dashed curves are evaluated from Eqs. (4) and (5). The $\Delta\nu_{1/2}$ expresses the second-order shift of the center line, and $\Delta\nu_m(m=\frac{3}{2}$ or $-\frac{3}{2})$ is the difference between the satellite frequency and the Larmor one, in the same way as $\Delta\nu$ in Fig. 2.

tive and negative $\Delta\nu$ were symmetrical with respect to $\nu_{l'0}$ within experimental errors.

The rotation pattern which will be ascribed to the satellites and the central line ($\Delta\nu_{1/2}$) of Cl ($A,A,0$), where $A=1,3,\ldots$ was observed as shown in Fig. 7.

In addition, the spectra for negative $\Delta\nu$ were checked and quadrupole spectra with positive and negative $\Delta\nu$ were asymmetrical with respect to the Larmor frequency of Cl which expresses an effect of the second-order perturbation due to the large quadrupole interaction. Since no other signals were observed in the range of $\Delta\nu=\pm 1.6$ MHz, the observed signal will be associated with the Cl (1,1,0). The angular variations of the quadrupole splittings of satellite lines in the first- and second-order perturbations[29,30] are given by

$$\begin{aligned}
\Delta\nu(E) &= \pm\nu_Q(1+\eta)(1-3\cos2\theta)/8+\tfrac{1}{192}(\nu_Q^2/\nu_L)[9(1+\eta)^2(1-\cos4\theta)+4(3-\eta)^2(1+\cos2\theta)]\ ,\\
\Delta\nu(F) &= \pm\nu_Q(1+\eta)(1+3\cos2\theta)/8+\tfrac{1}{192}(\nu_Q^2/\nu_L)[9(1+\eta)^2(1-\cos4\theta)+4(3-\eta)^2(1-\cos2\theta)]\ ,\\
\Delta\nu(G) &= \mp\nu_Q[(1+\eta)+(3-\eta)\sin2\theta]/4+\tfrac{1}{48}(\nu_Q^2/\nu_L)(3-\eta)^2(1+\cos4\theta)\ ,\\
\Delta\nu(J) &= \mp\nu_Q[(1+\eta)-(3-\eta)\sin2\theta]/4+\tfrac{1}{48}(\nu_Q^2/\nu_L)(3-\eta)^2(1+\cos4\theta)\ ,
\end{aligned}\tag{4}$$

where ν_L is the Larmor frequency of nucleus under study and equals $\nu_{l'0}$. The angular variation of the quadrupole shifts of central line in the second-order perturbation[29,30] will be

$$\begin{aligned}
\Delta\nu(K) &= (\nu_Q^2/1536\nu_L)\{-45(1+\eta)^2-16(3-\eta)^2-[36(1+\eta)^2-48(3-\eta)^2]\cos2\theta+81(1+\eta)^2\cos4\theta\}\ ,\\
\Delta\nu(M) &= (\nu_Q^2/1536\nu_L)\{-45(1+\eta)^2-16(3-\eta)^2+[36(1+\eta)^2-48(3-\eta)^2]\cos2\theta+81(1+\eta)^2\cos4\theta\}\ ,\\
\Delta\nu(N) &= (\nu_Q^2/384\nu_L)[18(1+\eta)^2-7(3-\eta)^2-12(3-\eta)(1+\eta)\sin2\theta-9(3-\eta)^2\cos4\theta]\ ,\\
\Delta\nu(P) &= (\nu_Q^2/384\nu_L)[18(1+\eta)^2-7(3-\eta)^2+12(3-\eta)(1+\eta)\sin2\theta-9(3-\eta)^2\cos4\theta]\ .
\end{aligned}\tag{5}$$

From the analysis of the spectra we obtain $\nu_Q=(972\pm2.0)$ kHz for ^{35}Cl and $\nu_Q=(762\pm2.0)$ kHz for ^{37}Cl and $\eta=0.102\pm0.005$ for both nuclei. From these results, the ratio of ν_Q^{37}/ν_Q^{35} is 0.784 which agrees with that of the nuclear quadrupole moments, Q^{37}/Q^{35}, the same value as that of Cl (1,1,0) sites in NaCl-Br in Sec. III A. Using Q^{37} and Q^{35}, we have the principal value of the EFG, $eq=339\times10^{12}$ esu/cm^3 with the same assignment of the principal axes as was obtained for Cl (1,1,0) in NaCl-Br.

C. NaI-Cl crystal

As shown in Fig. 8, the rotation pattern of the quadrupole spectra ascribed to Na (1,0,0) and Na (1,1,1) which are represented as A, B, C, and D, respectively, was obtained in the DNMR of NaI crystal containing 0.2 mole% Cl impurity ions, according to the analysis similar to that of Sec. III A. No other satellites were observed in the range of $\Delta\nu=\pm1.0$ MHz at $\theta=45°$.

From the analysis of the spectra we obtain $\nu_Q=(197.5\pm2.0)$ kHz for Na (1,0,0) and $\nu_Q=(120.0\pm2.0)$ kHz for Na (1,1,1). By using the Q for ^{23}Na, we have the principal values of the EFG, $eq=54\times10^{12}$ esu/cm^3 for Na (1,0,0) and 33×10^{12} esu/cm^3 for Na (1,1,1).

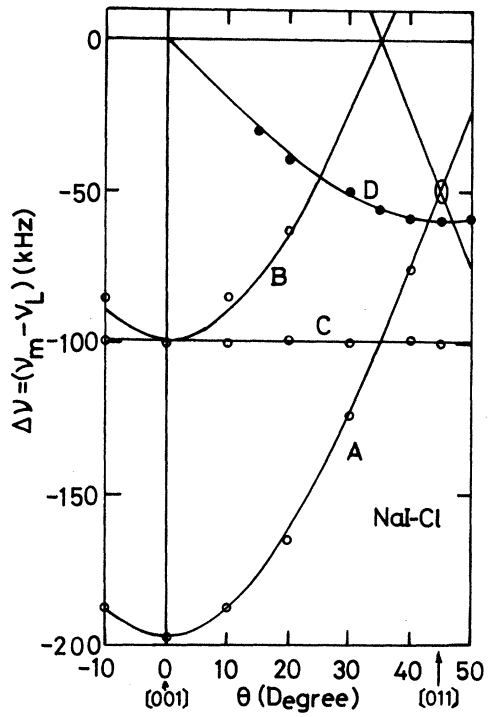

FIG. 8. Angular variation of the quadrupole spectra ascribed to Na (1,0,0) and (1,1,1) sites in NaI crystal containing 0.2 mole% Cl impurities. The solid curves are given by Eqs. (1) and (2).

D. NaBr-Cl crystal

As shown in Fig. 9, the angular dependence of the quadrupole spectra for the NaBr-Cl crystal was obtained. In these spectra, Na (1,0,0) and Na (1,1,1) are observed in which we obtain $\nu_Q = (127.0 \pm 2.0)$ and (80.0 ± 2.0) kHz for Na (1,0,0) and Na (1,1,1), respectively. Using the Q (^{23}Na) we have the principal values of EFG, $eq = 35 \times 10^{12}$ and 22×10^{12} esu/cm^3 for Na (1,0,0) and Na (1,1,1), respectively. However, ν_Q or eq of the present study for Na (1,0,0) in this crystal does not agree with the results of Kawamura *et al.*[4] ($eq = 96 \times 10^{12}$ esu/cm^3 at 300 K) and Andersson[11] ($\nu_Q = 248$ kHz at 300 k).

We have examined another rotation experiments of the same sites in same crystal. The angular variations of the quadrupole spectra in the rotation of the magnetic field H_0 about $[1\bar{1}0]$ direction in $(1\bar{1}0)$ plane are shown in Fig. 10 for same crystal. The angular variation of the quadrupole splittings of satellite lines in the first-order perturbation for (1,0,0) sites is given by

$$\Delta\nu(A) = \mp \nu_Q(1 + 3\cos 2\theta)/4 \ ,$$
$$\Delta\nu(B,C) = \pm \nu_Q(1 + 3\cos 2\theta)/8 \ , \qquad (6)$$

and also for (1,1,1) sites

$$\Delta\nu(D_1) = \mp \nu_Q(1 - \cos 2\theta + 2\sqrt{2}\sin 2\theta)/4 \ ,$$
$$\Delta\nu(D_2) = \mp \nu_Q(1 - \cos 2\theta - 2\sqrt{2}\sin 2\theta)/4 \ , \qquad (7)$$
$$\Delta\nu(D_3) = \pm \nu_Q(1 - \cos 2\theta)/4 \ .$$

The solid curves in Fig. 10 are obtained as the best fits with experimental frequencies by using Eqs. (6) and (7), assuming $\nu_Q = 127.0$ and 80.0 kHz for A, B, C, and D lines, respectively. Both ν_Q's are perfectly same as those of the rotation about [100] axis mentioned above. From these results, we confirm our assignments of A, B, C and D lines discussed above are correct.

The rotational patterns of the quadrupole splittings due to ^{79}Br (1,1,0) and ^{81}Br (1,1,0) in a NaBr crystal containing Cl^- impurity ions were observed as shown in Fig. 11, where both patterns are asymmetrical with respect to each Br Larmor frequency. From the analysis of the spectra we obtain $\nu_Q = (1400.0 \pm 2.0)$ kHz for ^{79}Br and $\nu_Q = (1190.0 \pm 2.0)$ kHz for ^{81}Br and $\eta = 0.103 \pm 0.006$ for both nuclei. From these results, the ratio ν_Q^{79}/ν_Q^{81} is 1.18 which agrees with that of the nuclear quadrupole moments, Q^{79}/Q^{81}. Using $Q^{79} = 0.33 \times 10^{-24}$ cm^2 and $Q^{81} = 0.28 \times 10^{-24}$ cm^2, we obtain the principal value of the EFG, $eq = 117 \times 10^{12}$ esu/cm^3 with the same assignment of

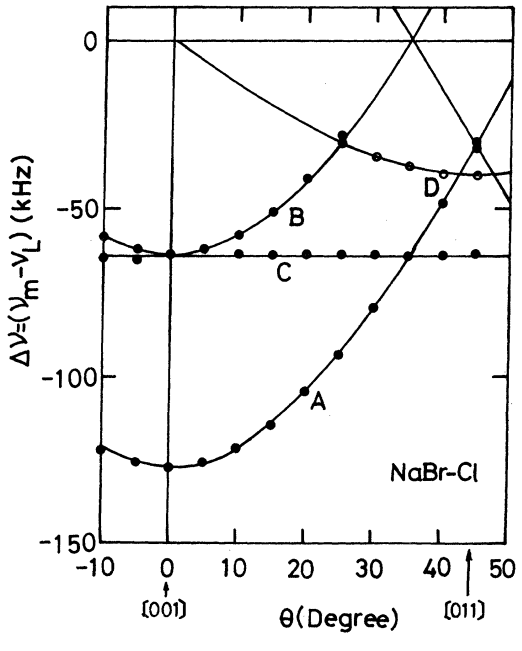

FIG. 9. Rotational pattern of the quadrupole spectra ascribed to Na (1,0,0) and (1,1,1) in NaBr crystal containing 0.2 mole% Cl impurities. The solid curves are calculated from Eqs. (1) and (2).

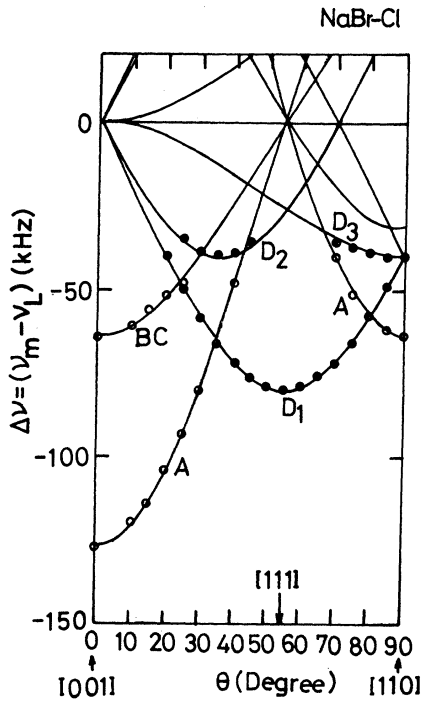

FIG. 10. Angular variation of the quadrupole spectra in NaBr-Cl crystal. The magnetic field H_0 was rotated about $[1\bar{1}0]$ direction in the $(1\bar{1}0)$ plane. The solid curves are given by Eqs. (6) and (7).

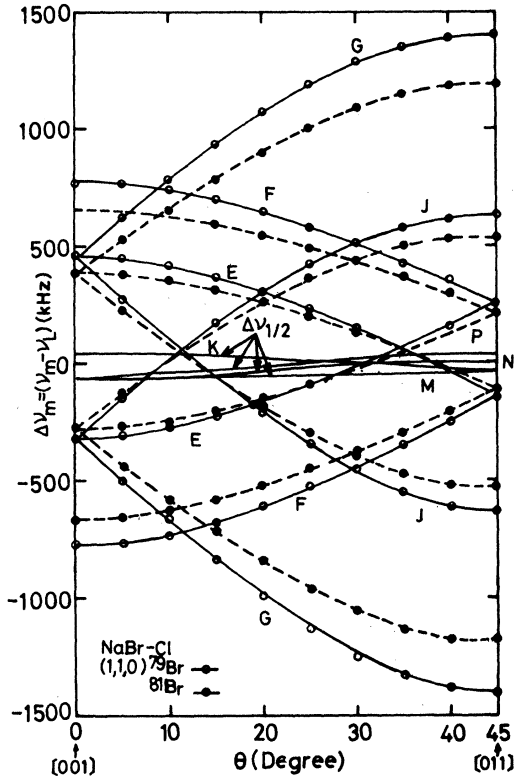

FIG. 11. Rotational pattern of the quadrupole spectra ascribed to Br (1,1,0) in NaBr-Cl crystal. The solid and dashed lines are given by Eqs. (4) and (5).

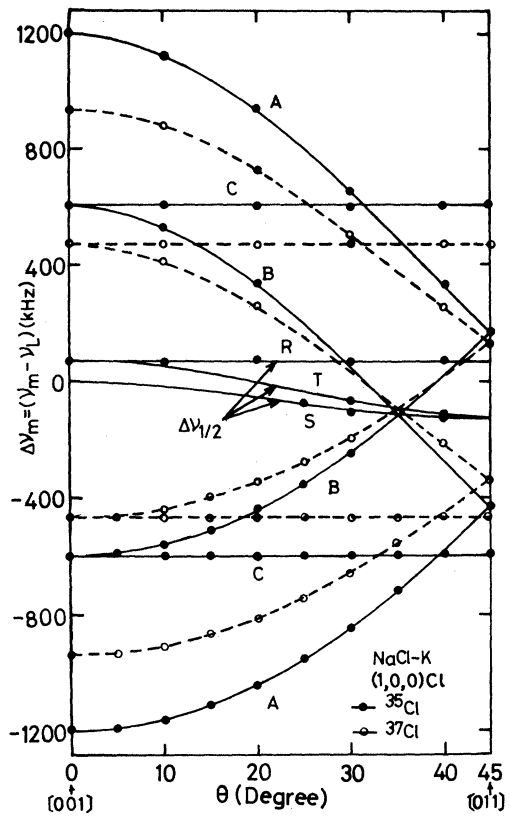

FIG. 12. Angular variation of the quadrupole spectra ascribed to Cl (1,0,0) in NaCl-K crystal containing 1.0 mole% K impurity ions. The solid and dashed lines are calculated from Eqs. (8) and (9).

the principal axes as was obtained for Cl (1,1,0) in NaCl-Br.

E. NaCl-K crystal

The quadrupole spectra of satellites and center lines ($\Delta\nu_{1/2}$) of ^{35}Cl (1,0,0) and ^{37}Cl (1,0,0) in K^+ impurity-doped NaCl crystals are obtained as shown in Fig. 12. Those of Na (1,1,0) and ^{35}Cl (1,1,1), ^{37}Cl (1,1,1) in the same crystals are also observed as shown in Figs. 13 and 14, respectively. The satellites of ^{35}Cl (1,0,0) and ^{37}Cl (1,0,0) are asymmetrical for each ν_L, while in Figs. 13 and 14 the symmetrical figures are observed.

The angular dependence of the quadrupole splittings of the satellite lines in the first- and second-order perturbations[29,30] will be calculated as follows:

$$\Delta\nu(A)=\mp\nu_Q(1+3\cos2\theta)/4 - \tfrac{3}{16}(\nu_Q^2/\nu_L)(1-\cos4\theta) \ ,$$

$$\Delta\nu(B)=\mp\nu_Q(1-3\cos2\theta)/4 - \tfrac{3}{16}(\nu_Q^2/\nu_L)(1-\cos4\theta) \ , \qquad (8)$$

$$\Delta\nu(C)=\pm\nu_Q/2 \ ,$$

and for the central line in the second-order perturbation,

$$\Delta\nu(R)=\tfrac{3}{16}(\nu_Q^2/\nu_L) \ ,$$

$$\Delta\nu(S)=\tfrac{3}{128}(\nu_Q^2/\nu_L)(-5-4\cos2\theta+9\cos4\theta) \ , \qquad (9)$$

$$\Delta\nu(T)=\tfrac{3}{128}(\nu_Q^2/\nu_L)(-5+4\cos2\theta+9\cos4\theta) \ .$$

From the analysis of the spectra, by using Eqs. (8), (9), (3), and (2) we have $\nu_Q=(1200.0\pm2.0)$, (950.0 ± 2.0), (350.0 ± 2.0), (280.0 ± 2.0), and (220.0 ± 2.0) kHz for ^{35}Cl (1,0,0), ^{37}Cl (1,0,0), ^{23}Na (1,1,0), ^{35}Cl (1,1,1), and ^{37}Cl (1,1,1) sites, respectively. In addition to these ν_Q values, $\eta=0.103\pm0.005$ for ^{23}Na (1,1,0) site is obtained from Fig. 13 and Eq. (3). The assignment of principal axes of the EFG in this site is the same as was obtained for Cl (1,1,0) sites in NaCl-Br. By using the values $Q(^{35}\text{Cl})$, $Q(^{37}\text{Cl})$, and $Q(^{23}\text{Na})$, we obtain the principal values of the EFG, $eq=421\times10^{12}$, 97×10^{12}, and 98×10^{12} esu/cm^3 for Cl (1,0,0), Na (1,1,0), and Cl (1,1,1), respectively.

Slusher and Hahn[28] obtained $\nu_Q=1197$, 944.5, 358, 280, and 220 kHz for ^{35}Cl (1,0,0), ^{37}Cl (1,0,0),

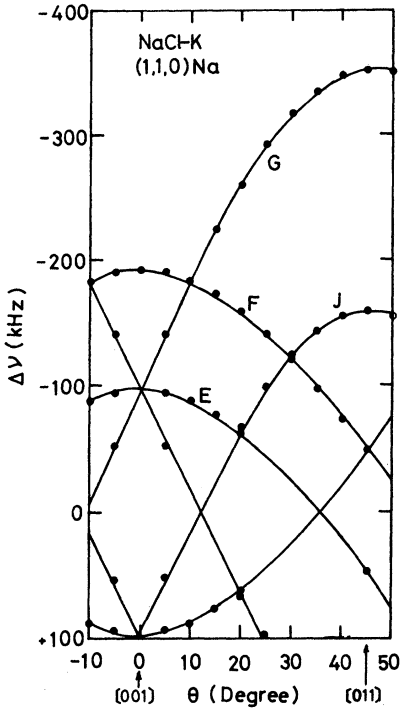

FIG. 13. Rotational pattern of the quadrupole spectra ascribed to Na (1,1,0) in NaCl-K crystal. The solid curves are given by Eq. (3).

^{23}Na (1,1,0), ^{35}Cl (1,1,1), and ^{37}Cl (1,1,1) in NaCl containing K^+ impurity ions by the PQR experiments, respectively. The values of ν_Q in the present study agree fairly well with their results.

F. NaBr-I crystal

The angular variations of quadrupole spectra of satellite lines ascribed to ^{23}Na (1,0,0) and ^{79}Br (1,1,0), ^{81}Br (1,1,0) in NaBr single crystals containing I^- impurity ions are observed as shown in Figs. 15 and 16, respectively. The satellite lines of ^{23}Na (1,0,0) and those of ^{79}Br (1,1,0), ^{81}Br (1,1,0) are asymmetrical for each ν_L as seen in both figures. The degree of asymmetry of ^{23}Na (1,0,0) is very small, but it is still beyond the experimental errors and agrees with the result of calculations.

By using the first- and second-order perturbations of Eqs. (8) and (4), we obtain the angular variations of the quadrupole splittings of satellite lines as shown on the solid or dotted lines of both figures where we have used $\nu_Q = (279.8 \pm 2.0)$, (3260.0 ± 2.0), and (2766.9 ± 2.0) kHz for ^{23}Na (1,0,0), ^{79}Br (1,1,0), and ^{81}Br (1,1,0), in order to get the best fits with the observed frequencies, respectively. But we could not observe the angular variations of the central lines in the ^{23}Na (1,0,0), ^{79}Br (1,1,0), and ^{81}Br (1,1,0) sites.

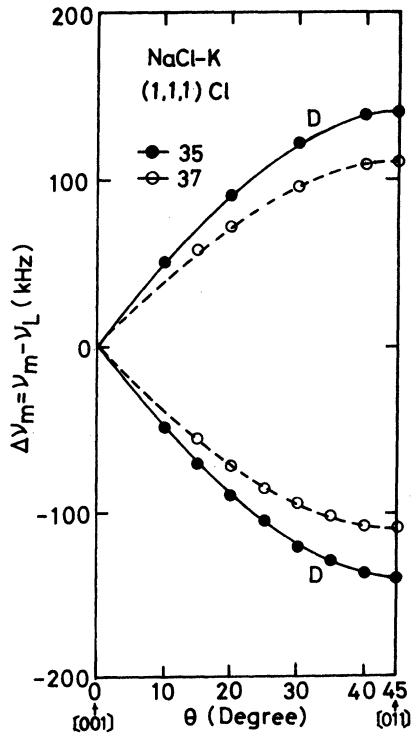

FIG. 14. Angular variation of the quadrupole spectra ascribed to Cl (1,1,1) in NaCl-K crystal. The solid and dashed lines are given by Eq. (2).

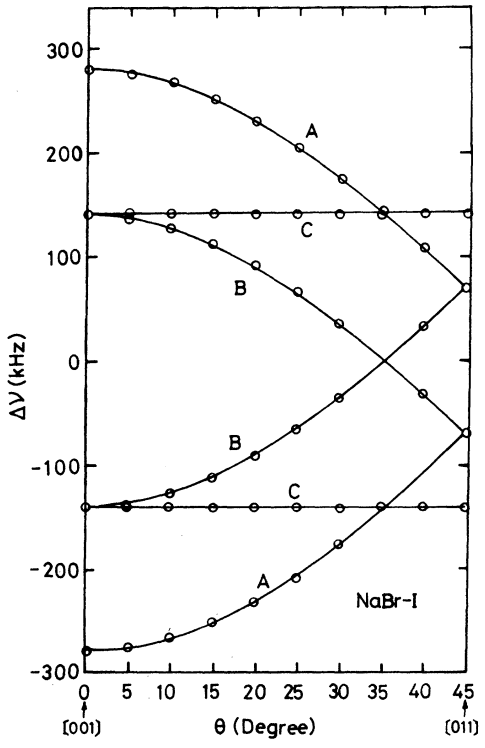

FIG. 15. Angular variation of the quadrupole spectra ascribed to Na (1,0,0) in NaBr-I crystal. The solid curves are given by Eq. (8) with $\nu_Q = 279.8$ kHz.

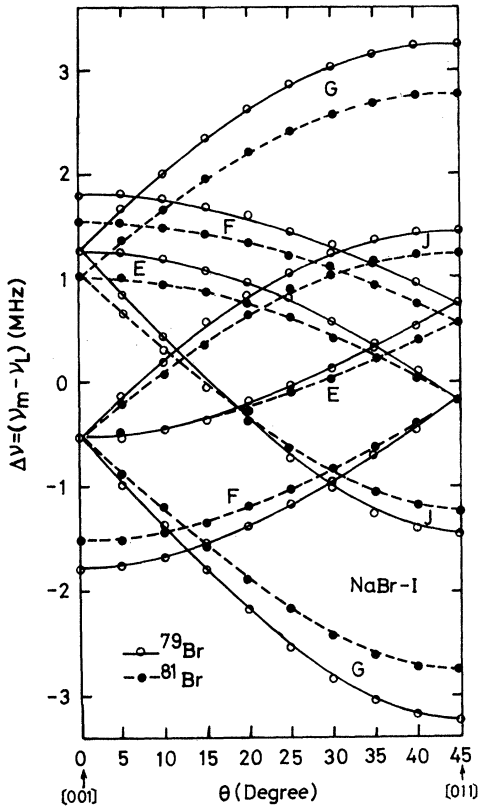

FIG. 16. Angular dependence of the quadrupole spectra ascribed to Br (1,1,0) in NaBr-I crystal. The solid and dashed lines are obtained by using Eq. (4) with $\nu_Q = 3260.0$ and 2766.9 kHz, respectively.

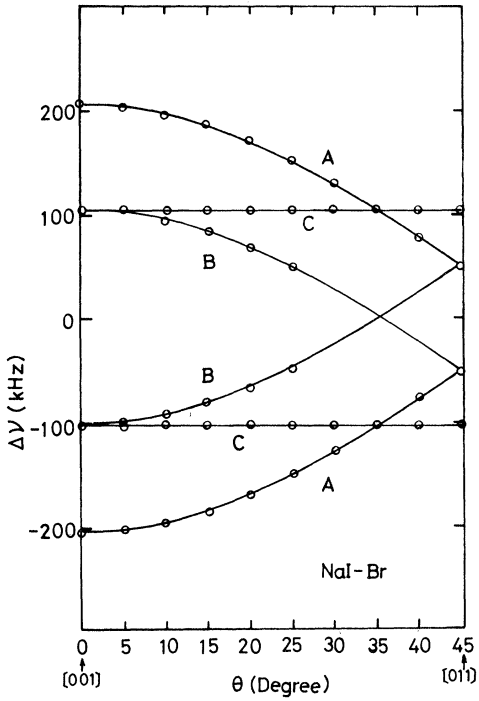

FIG. 17. Angular variation of the quadrupole spectra ascribed to Na (1,0,0) in NaI-Br crystal. The solid curves are given by Eq. (1) with $\nu_Q = 205.3$ kHz.

In addition to these ν_Q values, $\eta = 0.102 \pm 0.006$ for Br (1,1,0) is obtained from Fig. 16 and Eq. (4). The assignment of principal axes of the EFG in this site is the same as was obtained for Cl (1,1,0) in NaCl-Br. By using the values $Q(^{23}\text{Na})$, $Q(^{79}\text{Br})$, and $Q(^{81}\text{Br})$ we obtain the principal values of the EFG, $eq = 77.0 \times 10^{12}$ and 272.4×10^{12} esu/cm^3 for Na (1,0,0) and Br (1,1,0), respectively.

G. NaI-Br crystal

The quadrupole spectra of satellites of Na (1,0,0) in Br^- impurity-doped NaI crystals are obtained as shown in Fig. 17. The satellites of Na (1,0,0) are symmetrical for ν_L. The angular dependence of the quadrupole splittings of satellite lines in the first-order perturbation will be calculated as solid lines in Fig. 17 by using Eq. (1), where we have used $\nu_Q = (205.3 \pm 2.0)$ kHz for Na (1,0,0) in order to get the best fits with the observed values. Then the principal value of EFG at this site, $eq = 57 \times 10^{12}$ esu/cm^3 is obtained from this ν_Q and $Q(^{23}\text{Na})$ values.

IV. SUMMARY

The experimental values of ν_Q, $|eq|$, and η of this study are summarized in Table I and the ν_Q's are compared with Slusher and Hahn's PQR data.[28]

From the table, we can see first that ν_Q's of NaCl-Br and NaCl-K agree fairly well with those obtained by Slusher and Hahn[28] as mentioned previously. However, the data in this study are more accurate than theirs because in the pure quadrupole resonance only one resonance line is observed for one electron shell surrounding the impurity ion, while many lines can be measured separately by the angular variation of quadrupole splittings of the DNMR in high field. For (1,0,0)-type Na in NaCl-Br and NaBr-Cl crystals, the present study does not agree with results of Kawamura *et al.*[4] and those of Andersson.[11]

Secondly, it will be noted that all η's at (1,1,0) sites observed in this study have exactly the same value 0.10 within the experimental errors and the principal axes of the EFG at these sites have also the same directions, as described previously. On the other hand, the η values of (1,1,0) sites in several crystals containing monovalent impurity ions were measured by the observation of the second-order shifts in the central line or by using the DNMR experiments,

TABLE I. Experimental values of the quadrupole frequency and the principal value and the asymmetry parameter of the EFG.

Crystal	Site	ν_Q (kHz)	$\lvert eq \rvert$ (10^{12} esu/cm^3)	η	ν_Q[a] (kHz)
NaCl-Br$^-$	(1,0,0) ^{23}Na	187.7±2.0	52	0	*B* 191.5
	(1,1,0) ^{35}Cl	325.0±2.0	113	0.105±0.005	*E* 328.5[b]
	(1,1,0) ^{37}Cl	254.0±2.0			
	(1,1,1) ^{23}Na	140.0±2.0	39	0	*C* 259[b]
NaCl-I$^-$	(1,0,0) ^{23}Na	500.0±2.0	140	0	
	(1,1,0) ^{35}Cl	972.0±2.0	339	0.102±0.005	
	(1,1,0) ^{37}Cl	762.0±2.0			
	(1,1,1) ^{23}Na	330.0±2.0	91	0	
NaCl-K$^+$	(1,0,0) ^{35}Cl	1200.0±2.0	421	0	*H* 1197
	(1,0,0) ^{37}Cl	950.0±2.0			*G* 944.5
	(1,1,0) ^{23}Na	350.0±2.0	97	0.103±0.005	*F* 358
	(1,1,1) ^{35}Cl	280.0±2.0	98	0	*D* 280
	(1,1,1) ^{37}Cl	220.0±2.0			220
NaBr-Cl$^-$	(1,0,0) ^{23}Na	127.0±2.0	35	0	
	(1,1,0) ^{79}Br	1400.0±2.0	117	0.103±0.006	
	(1,1,0) ^{81}Br	1190.0±2.0			
	(1,1,1) ^{23}Na	80.0±2.0	22	0	
NaI-Cl$^-$	(1,0,0) ^{23}Na	197.5±2.0	54	0	
	(1,1,1) ^{23}Na	120.0±2.0	33	0	
NaBr-I$^-$	(1,0,0) ^{23}Na	279.8±2.0	77	0	
	(1,1,0) ^{79}Br	3260.0±2.0	272.4	0.102±0.006	
	(1,1,0) ^{81}Br	2766.9±2.0			
NaI-Br$^-$	(1,0,0) ^{23}Na	205.3±2.0	57	0	

[a]R. E. Slusher and E. L. Hahn, Phys. Rev. 166, 332 (1968). Letters *B*–*H* were defined by them.
[b]They did not identify *E* and *C* signals as ^{35}Cl (1,1,0) and ^{37}Cl (1,1,0) due to the reason of inadequate shapes of these signals as a function of the modulation frequency.

by the other workers,[9–12,17,19] and all η's were the values greater than 0.4 except one case of NaCl-Ag.[23]

In the forthcoming paper,[27] the *eq*, η, and the types of EFG tensors at (1,1,0) site classified by the directions of principal axes will be calculated and compared with the experimental results of this study and studies of other workers.

ACKNOWLEDGMENTS

The authors would like to thank Professor J. Itoh of Osaka University for valuable discussions. They are indebted to Professor H. Kanzaki of Institute for Solid State Physics, University of Tokyo for supplying the single crystals of NaCl-I.

*Portions of this paper are derived from the dissertation of T. Taki presented in partial fulfillment of the requirements for the degree of Doctor of Engineering, Osaka University.

[1]N. Bloembergen and T. J. Rowland, Acta Metall. 1, 731 (1953).
[2]N. Bloembergen, in *Defects in Crystalline Solids* (The Physical Society, London, 1955), p. 1.

[3]M. H. Cohen and F. Reif, in *Solid State Physics,* edited by F. Seitz and D. Turnbull (Academic, New York, 1957), Vol. 5.
[4]H. Kawamura, E. Otsuka, and K. Ishiwatari, J. Phys. Soc. Jpn. 11, 1064 (1956).
[5]E. Otsuka and H. Kawamura, J. Phys. Soc. Jpn. 12, 1071 (1957).
[6]V. V. Lemanov, Zh. Eksp. Teor. Fiz. 40, 775 (1961) [Sov. Phys. JETP 13, 543 (1961)].
[7]M. Kornfeld and V. V. Lemanov, Zh. Eksp. Teor. Fiz. 41, 1454 (1961) [Sov. Phys. JETP 14, 1038 (1962)].
[8]Y. Fukai, J. Phys. Soc. Jpn. 18, 1413 (1963); 18, 1580 (1963).
[9]L. O. Andersson and E. Forslind, Ark. Fys. 28, 49 (1964); L. O. Andersson and L. Ödberg, *ibid.* 35, 85 (1967).
[10]L. O. Andersson, in *Magnetic Resonance and Relaxation,* edited by R. Blinc (North-Holland, Amsterdam, 1967), p. 1101.
[11]L. O. Andersson, Helv. Phys. Acta 41, 414 (1968); Ark. Fys. 40, 71 (1969).
[12]W. D. Ohlsen and M. E. Melich, Phys. Rev. 144, 240 (1966).
[13]S. R. Hartmann and E. L. Hahn, Phys. Rev. 128, 2042 (1962).
[14]F. M. Lurie and C. P. Slichter, Phys. Rev. 133, A1108 (1964).
[15]R. E. Slusher and E. L. Hahn, Phys. Rev. Lett. 12, 246 (1964).
[16]A. G. Redfield, Phys. Rev. 130, 589 (1963).
[17]A. Hartland, Proc. R. Soc. London, Ser. A 304, 361 (1968).
[18]G. T. Mallick, Jr., and R. T. Schumacher, Phys. Rev. 166, 350 (1968).
[19]K. F. Nelson and W. D. Ohlsen, Phys. Rev. 180, 366 (1969).
[20]D. A. McArthur, E. L. Hahn, and R. E. Walstedt, Phys. Rev. 188, 609 (1969).
[21]P. R. Spencer, H. D. Schmid, and C. P. Slichter, Phys. Rev. B 1, 2989 (1970).
[22]D. V. Lang and P. R. Moran, Phys. Rev. B 1, 53 (1970); 2, 2360 (1970).
[23]W. J. Meyer, D. V. Lang, and C. P. Slichter, Phys. Rev. B 8, 1924 (1973).
[24]M. Kunitomo, J. Phys. Soc. Jpn. 30, 1059 (1971).
[25]T. Taki, T. Kanashiro, T. Ohno, and M. Satoh, J. Phys. Soc. Jpn. 34, 558 (1973); T. Taki and M. Satoh, *ibid.* 36, 312 (1974); 38, 289 (1975); 38, 291 (1975); Phys. Status Solidi B 71, K21 (1975).
[26]T. Taki, T. Kanashiro, T. Ohno, and M. Satoh, J. Phys. Soc. Jpn. 36, 470 (1974); T. Taki, Ph.D. dissertation (Osaka University, 1975) (unpublished).
[27]M. Satoh and T. Taki, Phys. Rev. B 23, 6732 (1981) (following paper).
[28]R. E. Slusher and E. L. Hahn, Phys. Rev. 166, 332 (1968).
[29]G. M. Volkoff, Can. J. Phys. 31, 820 (1953).
[30]G. M. Volkoff, H. E. Petch, and D. W. L. Smellie, Can. J. Phys. 30, 270 (1952).